

Case Report

Multimodality Imaging and Multidisciplinary Approach to Post–Myocardial Infarct Ventricular Septal Defect Management

Max Puthenpura, MD, Joseph Kassab, MD, Joanna Ghobrial, MD, Aaron Weiss, MD, Serge C. Harb, MD, and Rohit Moudgil, MD

Heart, Vascular and Thoracic Institute, Cleveland Clinic Foundation, Cleveland, Ohio, USA

Interventricular septal rupture is a critical complication of acute myocardial infarction (MI).¹ It almost always has symptoms, from exertional dyspnea to severe cardiogenic shock.² Predictors of worse outcomes include female gender, advanced age, hemodynamic compromise, and delayed management.¹ Although surgical repair remains the gold standard for treatment, it is still associated with a high mortality rate.³ This case describes a patient who presented with an asymptomatic post-anterior MI ventricular septal defect (VSD) whose treatment was guided by advanced imaging and 3D remodelling modalities.

Case Presentation

A 71-year-old woman with a history of hypertension and rheumatoid arthritis initially presented to an outside hospital for indigestion and heartburn that had started earlier that morning. Chest X-ray and abdominal exam were grossly unremarkable. A same-day electrocardiogram showed concern for an ST-elevation myocardial infarction (STEMI) in the anterolateral leads (Supplemental Fig. S1). Troponin levels peaked to 11,252.80 pg/mL² (normal: 10.10–27.10 pg/mL²). The patient underwent catheterization, which demonstrated a near-complete stenosis estimated at 99% of the mid-left anterior descending (LAD) coronary artery. She was treated with balloon angioplasty and placement of a drug-eluting stent (Supplemental Fig. S2). She recovered and remained stable. However, next-day follow-up trans-thoracic echocardiography (TTE) demonstrated a post-MI VSD distal to the anteroseptal area with left-to-right shunting. She was asymptomatic, without any shortness of breath or chest pain. She was subsequently referred to the


Cleveland Clinic for further management and presented there 4 days after her initial MI.

Upon admission, the patient's vital signs were stable, demonstrating a blood pressure of 116/73 mm Hg, pulse of 76 beats per minute, temperature of 36.3°C, and an oxygen saturation of 99% on room air at 18 respirations per minute. Her admission labs of complete blood counts, complete metabolic panel, and magnesium levels demonstrated hyponatremia to 131 mmol/L and albumin to 3.6 g/dL, with all other values within normal limits. Physical exam demonstrated a 3/6 holosystolic murmur on the left lower sternal border, clear lungs to auscultation bilaterally, no leg edema, palpable peripheral pulses, and generally no acute distress.

Differential diagnosis

This atypical presentation of a VSD was most likely related to the recent MI. Other possibilities, such as a congenital cause, mitral regurgitation due to recent ischemia, as well as contained free wall rupture were less-likely differentials.

Investigation

Initial cardiac workup started with an admission electrocardiogram illustrating normal sinus rhythm with right axis deviation (Supplemental Fig. S3). TTE (Fig. 1; Video 1 , view video online) demonstrated the known apical VSD of 0.8 cm. The estimated ratio of total pulmonary blood flow to total systemic blood flow (Q_p/Q_s) was 1.41, consistent with the left-to-right shunting. Left ventricle thickness and systolic function were normal, with an ejection fraction of 59%. However, grade 1 left ventricular diastolic dysfunction along with left atrial dilation were identified. A mild pericardial effusion was noted in the parasternal long-axis view (Fig. 1). Right heart catheterization later showed preserved cardiac index by thermodilution of 3.48 L/min per m², pulmonary capillary wedge pressure of 20 mm Hg, right atrial pressure of 12 mm Hg, and mean pulmonary arterial pressure of 32 mm Hg. An O₂ saturation step up was noted from right atrial (RA) to right ventricular (RV; RA 66%, RV 89%, pulmonary arterial [PA]

Received for publication June 26, 2023. Accepted September 9, 2023.

Corresponding author: Dr Rohit Moudgil, Cleveland Clinic, J2-134, J2-4 Desk, 9500 Euclid Avenue, Cleveland, Ohio 44195, USA. Tel.: +1-216-445-1932; fax: +1-216-636-6962.


E-mail: moudgir@ccf.org

See page 937 for disclosure information.

Novel Teaching Points

1. Maintaining a high index of suspicion for post MI-VSD in patients with the described risk factors (age, female, hypertension, nonsmoker, anterior MI, subtotal occlusion) is crucial, as this condition can sometimes be asymptomatic, and lack of treatment is associated with extremely high rates of mortality.
2. In hemodynamically stable patients, multimodality cardiac imaging can help operators better visualize and understand complicated VSD anatomy and plan the optimal intervention in advance

78%, pulmonary capillary wedge pressure 96%), consistent with the diagnosis of post MI VSD. An injected 4D cardiac computed tomography (CT) scan with multiplanar reconstruction was done to further visualize anatomy (Fig. 2). The scan demonstrated a left apical ventricular septal defect with a large (3.1×1.7 cm in systole; 3.9 cm^2 area and 2.6×1.02 cm in diastole, 2.07 cm^2 area) opening on the left ventricular side of the septum, multiple apical RV muscle bundles partially occluding the defect with a small communication into the apical RV space (1.0×0.7 cm). Both ventricles were normal in size. 3D printing of the defect using segmentation, software planning, and a Stratasys J750 multi-material polyjet technology 3D printer (Stratasys Eden, Prairie, MN) were done to

clarify the anatomy of the defect (Fig. 2F; Video 2 , view video online).

Management

The management team involved structural and interventional cardiology, cardiac surgery, advanced imaging, and the primary cardiology team. A transcatheter closure (TCC) was initially considered. However, due to the apical nature and size of the defect, the determination was made that the percutaneous device would not tether well to the myocardial wall around the apical defect. This issue was illustrated succinctly in the 3D modelling that helped illustrate the complexity of the orifice and aided in planning for the procedure. Features of the defect included pulmonary hypertension and a high orifice area not amenable to transcatheter tethering. Thus, the patient was recommended for surgical management, including VSD repair and a coronary artery bypass graft with saphenous vein graft (SVG) to the LAD. The coronary artery bypass graft was deemed necessary due to complex vessel coronary artery disease even after percutaneous coronary intervention. The SVG was chosen instead of a left interior mammary artery graft, owing to concern for competitive flow from the high flow rate of the left interior mammary artery graft and the still-patent LAD. The intervention was carried out 14 days after the MI. Procedural guidance with 3D transesophageal echocardiography with multiplanar reconstruction highlighted the oval-shaped

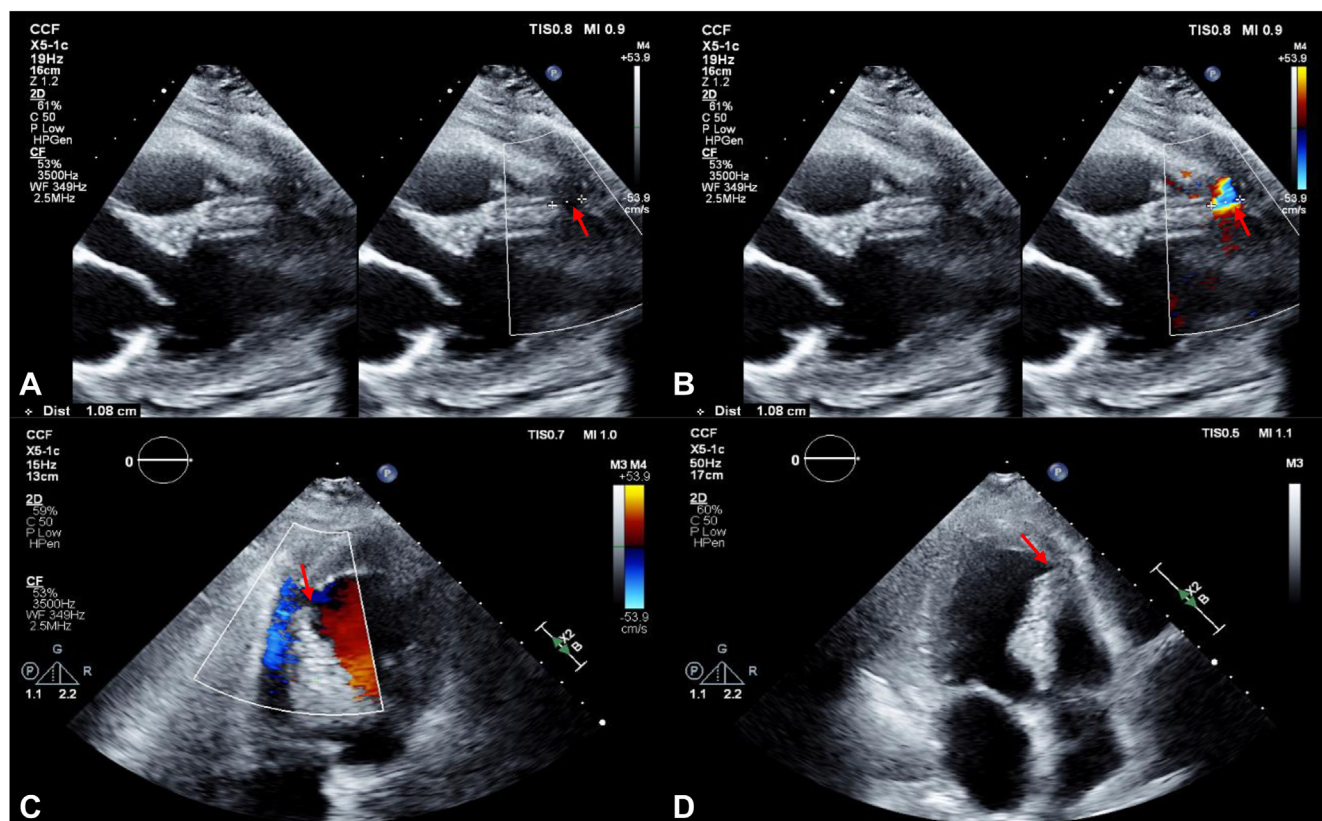


Figure 1. Transthoracic echocardiogram. (A) Parasternal long-axis view showing the ventricular septal defect (VSD) of interest (red arrow). (B) Left-to-right shunting illustrated with color Doppler flow (red arrow). (C) Parasternal short-axis view of the VSD (red arrow). (D) A 4-chamber view showing another angle of the VSD (red arrow).

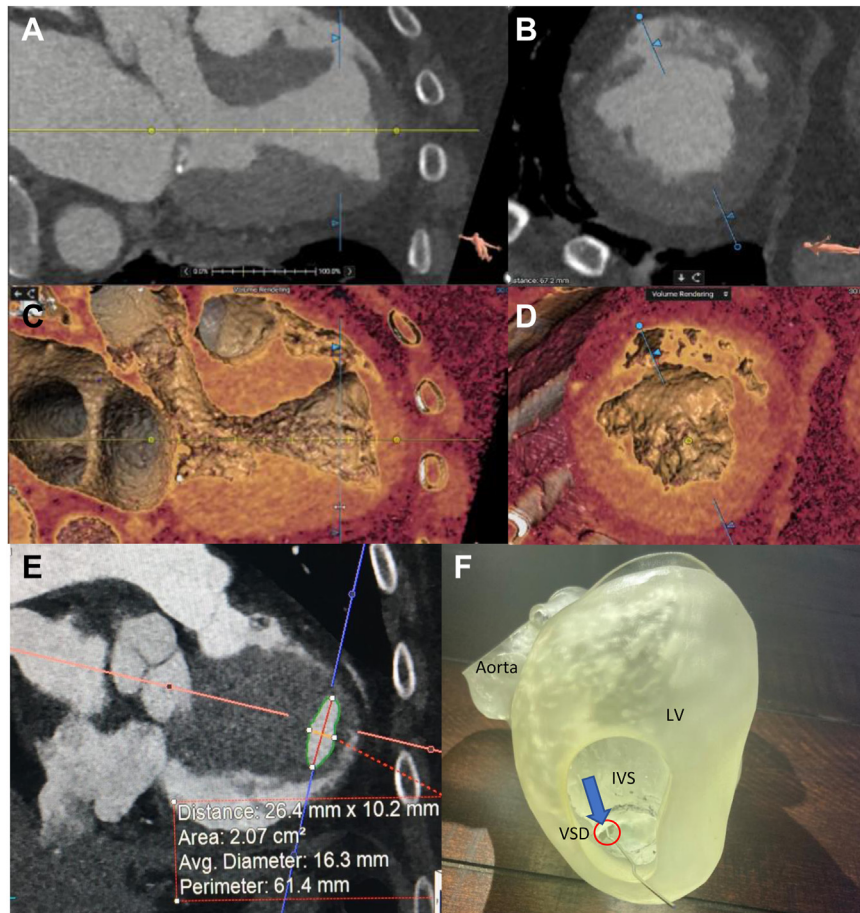


Figure 2. Four-dimensional (4D) cardiac computed tomography image with multiplanar reconstruction (MPR) and 3D printing. **(A)** A preoperative long-axis MPR of the ventricular septal defect (VSD; **blue arrow**). **(B)** A preoperative short-axis MPR of the VSD (**blue arrow**). **(C)** A preoperative long-axis 3D rendering of the VSD (**blue arrow**). **(D)** A preoperative short-axis 3D rendering of the VSD (**blue arrow**). **(E)** A 2D preoperative computed tomography image of the VSD (**blue arrow**). **(F)** A 3D-printed model of the VSD with left ventricular (LV) window (**blue arrow**; wire indicating VSD tract). IVS, intact ventricular septum.

anterior-apical VSD. Estimated measurements were 3.76×1.65 cm, with an area of 3.81 cm², with the larger orifice on the left side of the defect, consistent with pre-procedural cardiac CT imaging (Supplemental Fig. S4; Video 3 [view video online](#)). After sternotomy, the defect first was assessed through the tricuspid valve, but its location was too deep to safely suture. Therefore, a right ventriculotomy was done, with closure of the VSD using 3 interrupted pledgeted sutures. The SVG-to-LAD bypass was then performed, with trivial residual flow on transesophageal echocardiography. The patient was later extubated the same day without complications.

The patient was discharged and was seen a month later for follow-up. She had no complaints and was recovering well. However, a small residual apical VSD with trivial left-to-right shunting and mild pulmonary hypertension (RV systolic pressure 41 mm Hg) were denoted on follow-up TTE (Supplemental Fig. S5). Given the lack of concerning symptoms during the follow-up visit, with stable residual defect size, interval imaging was deemed appropriate for management and she was advised to follow up in 6 months.

Discussion

This case illustrates an unusual presentation of a rare post-MI complication. Mechanical complications of acute MI occur in about 3 per 1000 patients, with most of these events occurring with ST-elevation myocardial infarction.¹ Patients developing this condition are more likely to be female, of older age, suffering from an anterior MI, with high blood pressure, and nonsmokers.² Furthermore, the risk is increased with complete occlusion of the infarct-related artery.³ Notably, this patient had almost all of these risk factors. Patients with post-MI VSD are typically symptomatic, with symptoms ranging from exertional dyspnea to severe cardiogenic shock.⁵ In contrast, this patient presented with an asymptomatic systolic murmur and excellent hemodynamics. In addition, she did not demonstrate expected symptoms, such as dyspnea from pulmonary edema, chest pain from coronary malperfusion, or hemodynamic compromise from her VSD. This lack of symptoms could be due to her preserved ejection fraction on presentation, and the degree of intracardiac shunting not being strong enough to decompensate her hemodynamics. Having her initial coronary event addressed likely resolved the myocardial irritation that caused her initial indigestion.

Although VSD is rare, a high index of suspicion for VSD should be kept in patients presenting with risk factors.

Imaging modalities play a central role in management. Although diagnosis is usually established by TTE, this patient had a 4D cardiac CT scan with multiplanar reconstruction, and a 3D-printed reconstruction of her VSD that helped the team decide on surgery. Aside from guiding management, advanced imaging helped delineate the true anatomy of the defect. 2D-TTE measured the defect at 0.8 cm, and high-definition 4D CT and 3D printing demonstrated an average diameter of 1.6 cm in diastole (Fig. 2). This large incongruence is likely explained by the ellipsoid shape, which may have been measured off axis by initial imaging. Understanding the extent of the defect helped in the decision to use surgical intervention rather than TCC.

In atypical presentations and stable patients, advanced imaging demonstrates a unique role in defining the treatment course. Other modalities, such as 3D TTE, could have been used for further evaluation. However, the added utility was limited given that the initial TTE assessment with follow-up advanced imaging and 3D printing offered enough information for management. Cardiac magnetic resonance imaging could have been utilized to better assess the infarct area and reevaluate the shunt fraction for more comprehensive management. However, much of the myocardium likely had completed infarction, and precisely defining this territory was not critical for management of the case. In light of pursued comprehensive investigations, the decision was made not to obtain cardiac magnetic resonance imaging.

Without repair, the post-MI VSD mortality rate is as high as 90% within 2 months.⁴ Therefore, diagnosis should prompt expedited discussion and intervention. Studies have shown lower mortality rates in patients who underwent repair several weeks after MI, compared to those who received earlier management. This difference could be due to the infarcted myocardium being weak initially after MI. Early intervention could predispose the heart to recurrent VSD. Delaying the procedure allows the friable tissue to organize and differentiate itself from the surrounding healthy tissue.⁵ However, selection bias in surgical outcomes may be present, as patients with preserved left ventricular function are chosen as low-risk surgical candidates.⁵ Nevertheless, repair should happen, as untreated patients might progress to decompensated heart failure and multiorgan failure.⁵⁻⁷ The timing of surgery in the context of post-MI VSD should be individualized. In this patient, the repair was performed 14 days after the diagnosis of MI. This timing allowed for an adequate clopidogrel washout and sufficient tissue maturation. In tandem, we aimed to avoid risking sudden hemodynamic compromise, which can happen in patients who present as hemodynamically stable.⁵⁻⁷

Increasing evidence supports the use of percutaneous TCC, especially in critically ill patients or those suffering from multiple comorbidities. This approach also can provide early hemodynamic stabilization, allowing for tissue healing prior to surgical closure. TCC can definitively treat hemodynamically stable patients who have anatomically suitable defects (ie, defect size < 15 mm), and subacute to chronic post-MI VSD (> 3.5 weeks).⁷ In this case, given the suboptimal anatomy (ellipsoid shape), size (> 15 mm), and location (apical) of the defect, surgical management was

deemed superior to percutaneous closure. This decision was made possible with the advanced imaging modalities employed in the management of the case.

Conclusion

This atypical case reinforces the importance of standardized follow-up imaging in post-MI patients. The imaging and 3D printing of the complex anatomy of the defect illustrates how advanced cardiac imaging helps guide decisions in choosing appropriately between TCC and surgical management.

Ethics Statement

The authors confirm that all protected health information has been withheld from publication.

Patient Consent

The authors confirm that a patient consent form was obtained for this article.

Funding Sources

The authors have no funding sources to declare.

Disclosures

The authors have no conflicts of interest to disclose.

References

1. Reeder GS. Identification and treatment of complications of myocardial infarction. *Mayo Clin Proc* 1995;70:880-4.
2. Crenshaw BS, Granger CB, Birnbaum Y, et al. Risk factors, angiographic patterns, and outcomes in patients with ventricular septal defect complicating acute myocardial infarction. GUSTO-I (Global Utilization of Streptokinase and TPA for Occluded Coronary Arteries) Trial Investigators. *Circulation* 2000;101:27-32.
3. Radford MJ, Johnson RA, Daggett WM, et al. Ventricular septal rupture: a review of clinical and physiologic features and an analysis of survival. *Circulation* 1981;64:545-53.
4. American College of Cardiology. Contemporary management of post-MI ventricular septal rupture. Available at: <https://www.acc.org/latest-in-cardiology/articles/2018/07/30/06/58/contemporary-management-of-post-mi-ventricular-septal-rupture>. Accessed July 31, 2023.
5. Arnaoutakis GJ, Zhao Y, George TJ, et al. Surgical repair of ventricular septal defect after myocardial infarction: outcomes from the Society of Thoracic Surgeons National Database. *Ann Thorac Surg* 2012;94:436-43. discussion 443-4.
6. Jones BM, Kapadia SR, Smedira NG, et al. Ventricular septal rupture complicating acute myocardial infarction: a contemporary review. *Eur Heart J* 2014;35:2060-8.
7. Attia R, Blauth C. Which patients might be suitable for a septal occluder device closure of postinfarction ventricular septal rupture rather than immediate surgery? *Interact Cardiovasc Thorac Surg* 2010;11:626-9.

Supplementary Material

To access the supplementary material accompanying this article, visit *CJC Open* at <https://www.cjcopen.ca/> and at <https://doi.org/10.1016/j.cjco.2023.09.004>.